

Taking into consideration the efficiency of hydrated electron reactivity with Au^{3+} (eq 5) in the microemulsion, the Au^{2+} formed is estimated to be 2.6×10^{-6} M. Thus, each microemulsion droplet contains less than one molecule of Au^{2+} . Under this condition Au^{2+} disproportionation (reaction 5) primarily occurs through the exchange of the contents of neighboring microemulsions.²¹ It has been shown in several studies on the self-diffusion coefficients of water in microemulsions²⁹ that the diffusion coefficient is about 1 order of magnitude less than that in pure water. Since dissolved Au^{2+} in the microemulsion can be expected to follow the water, the experimentally determined ratio of rate constants for reaction 5 (k_5) in the two solvent systems agrees fairly well with the calculated diffusion coefficient ratio.

The size of microemulsion droplet also limits the size of gold colloids if Poisson's distribution prevails. Since surfactant-entrapped water molecules exchange on the millisecond time scale,³⁰ formation of larger colloidal particles are possible by aggregation of neutral gold atoms from different droplets. Growth is ultimately limited by statistical considerations. The rate of reduction has been shown to affect profoundly the morphology and hence the catalytic efficiency of colloidal metal particles.⁵ High-energy laser pulses on electrons provide means for controlling the rates of colloidal growth and hence open the door to systematic investi-

gations. The role of microemulsions is to compartmentalize desired amounts of Au^{3+} . Kinetic confinements within a water pool facilitate nucleation and limit the growth of gold colloids. Formation of uniform well-separated particles is an additional advantage of preparing metal colloids in the restricted environments of surfactant aggregates. Indeed, information could be obtained on the arrangements of atoms by lattice-imaging techniques in colloidal gold particles prepared by reducing Au^{3+} ions in liposomes. Conversely, no atomic arrangement could be discerned in particles prepared in homogeneous solutions.³¹ Organized assemblies provide, therefore, a means for the in-depth investigation of uniquely arranged subcolloidal particles. Extension of this principle to catalytically active colloids is the subject of our current attention.

Acknowledgment. Support of this work by the Department of Energy (J.H.F.) and the Swedish Natural Research Council (P.S.) are gratefully acknowledged. Pulse radiolysis experiments were carried out at the Center for Fast Kinetic Research, University of Texas, Austin, TX. This facility is supported by NIH Grant RR-00886 from the Biotechnology Branch of the Division of Research Resources and by the University of Texas. We appreciate the competent technical assistance of Wayne Reed.

Registry No. Au, 7440-57-5; HAuCl_4 , 16903-35-8.

(30) Lindman, B.; Stilbs, P.; Mosely, M. E. *J. Colloid Interface Sci.* **1981**, *83*, 569.

(31) R. J. P. William, private communication, 1982.

Proton-Exchange Rates in Solid Tropolone As Measured via ^{13}C CP/MAS NMR[†]

Nikolaus M. Szeverenyi, Ad Bax, and Gary E. Maciel*

Contribution from the Department of Chemistry, Colorado State University, Fort Collins, Colorado 80523. Received October 5, 1982

Abstract: The rate of proton exchange is measured for solid tropolone in a new type of ^{13}C CP/MAS NMR experiment. The analysis of the ^{13}C NMR data in conjunction with previous X-ray results suggests that the exchange rate is determined by the reorientation of the molecule in the lattice, involving an energetically unfavorable "out-of-plane" rotation to restore proper lattice packing.

Introduction

There has been considerable interest in a class of molecules having hydrogen bonding with a double-well potential. One such molecule, tropolone (2-hydroxy-2,4,6-cycloheptatrien-1-one), has recently been shown by a two-dimensional (2-D) NMR experiment to interconvert between two equivalent structures in the solid state.¹ This exchange can be represented as shown in Figure 1. In this paper we wish to report measurements of the proton exchange rate as a function of temperature and describe the new nmr experiment by which these data were obtained.

When examined as a liquid above its melting temperature (50–51 °C) in an ordinary ^{13}C NMR experiment, tropolone gives four sharp resonance signals, as shown in Figure 2a. This spectrum reflects the rapid interconversion shown in Figure 1 and results in the averaging of resonance positions for carbons C-1 with C-2, C-3 with C-7, and C-4 with C-6. The solid-state ^{13}C NMR spectrum obtained at room temperature by the conventional cross polarization/magic angle spinning technique (CP/MAS),² however, does not display this averaging behavior. Each individual carbon type, e.g., the carbonyl, the hydroxyl-bearing carbon, etc.,

are seen as individual resonances (Figure 2b). Even as the temperature is increased in the solid-state experiment, the peak positions and line widths are found to be unaffected. In a similar experiment with the compound naphthazarine, Shiao et al. have observed ^{13}C CP/MAS NMR spectra for both the nonexchanging and the exchanging system at different temperatures.³

Examination of tropolone at 35 °C via a 2-D ^{13}C NMR experiment on the solid yields a mapping out of the exchange network and facilitates the assignment of chemical shifts. Figure 3 shows the contour plot for such an experiment. This experiment is described in detail in ref 1 and is analogous to that proposed by Jeener and co-workers⁴ for mapping out chemical-exchange networks in liquid samples. Suter and Ernst⁵ have also used the

(1) N. M. Szeverenyi, M. J. Sullivan, and G. E. Maciel, *J. Magn. Reson.* **47**, 462 (1982).

(2) (a) A. Pines, M. G. Gibby, and J. S. Waugh, *J. Chem. Phys.*, **59**, 569 (1973). (b) J. Schaefer and E. O. Stejskal, *J. Am. Chem. Soc.*, **98**, 1031 (1976).

(3) W.-I. Shiao, E. N. Duesler, I. C. Paul, D. Y. Curtin, W. G. Blann, and C. A. Fyfe, *J. Am. Chem. Soc.*, **102**, 4546 (1980).

(4) J. Jeener, B. H. Meier, P. Bachmann, and R. R. Ernst, *J. Chem. Phys.*, **71**, 4546 (1979).

(5) D. Suter and R. R. Ernst, *Phys. Rev. B*, **25**, 6038 (1982).

[†] Presented in part at the 23rd Experimental NMR Conference, Madison, WI Apr 1982.

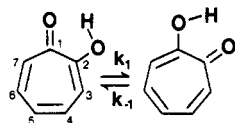


Figure 1. Chemical exchange involving the transfer of a proton in the hydrogen-bonded molecule, tropolone.

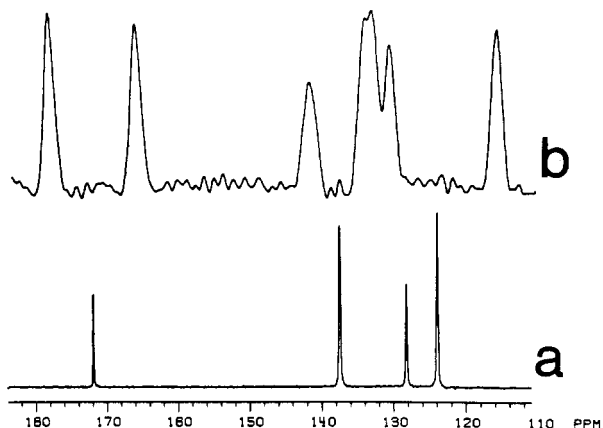


Figure 2. Comparison of the ^{13}C NMR spectrum of tropolone in the liquid and solid state. The liquid-state spectrum (a) was obtained at 60 $^{\circ}\text{C}$ on the pure molten material, while the solid-state spectrum (b) was obtained in a conventional CP/MAS experiment at room temperature.

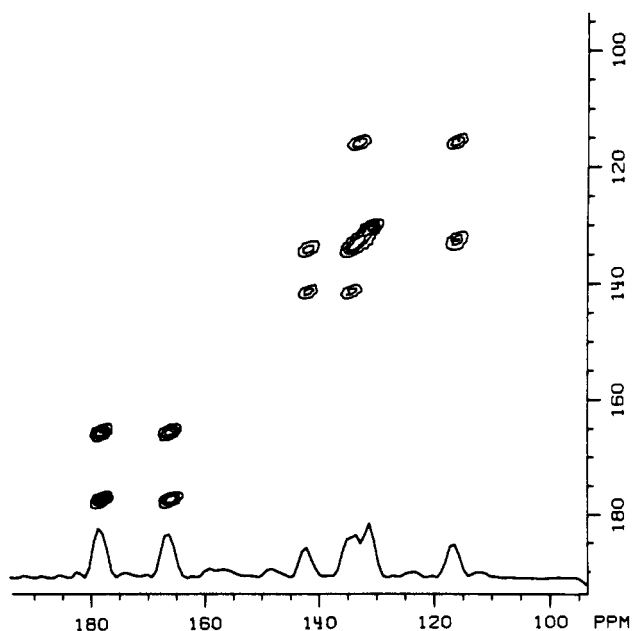


Figure 3. Chemical-exchange network in tropolone mapped out in a 2-D ^{13}C NMR experiment.¹ The spectrum was obtained at 35 $^{\circ}\text{C}$ with a mixing time of 6 s.

cross-polarization version of this 2-D experiment to study spin diffusion in solids. Briefly, the experiment involves labeling each ^{13}C spin isochromat and observing how this magnetization label is redistributed during the mixing period that follows. In the absence of any exchange process, peaks are observed only along the diagonal in the 2-D spectrum. The presence of cross-peak intensity indicates that during the mixing period exchange has occurred involving the sites with chemical shifts connected by the cross peaks. The intensity of the cross peaks is determined by the exchange rate and the length of the mixing period. It can be seen in Figure 3 that the carbonyl (C-1) peak (178.1 ppm) shares cross-peak intensity with the hydroxyl-bearing carbon (C-2) peak (166.0 ppm). Cross-peak intensity reflects exchange between these sites. Likewise cross-peak intensity is seen for the other carbon pairs (C-3 with C-7 and C-4 with C-6). The C-5 resonance (131 ppm) is not affected by the exchange, as can be rationalized

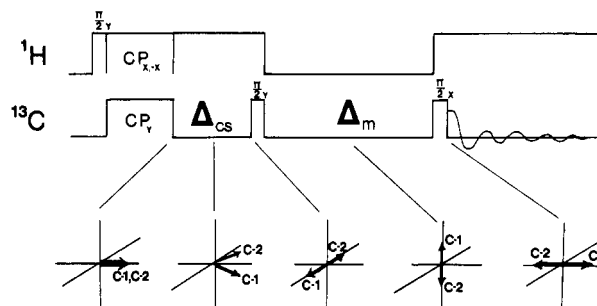


Figure 4. Pulse diagram and corresponding vector picture of ^{13}C magnetization for the ^{13}C NMR experiment used in obtaining exchange information.

by the scheme shown in Figure 1, and correspondingly communicates with no other site in the 2-D experiment. As exchange rates are rather difficult to extract from the 2-D data, an improved experiment was designed to measure this exchange rate and is described below.

Experimental Section

The NMR experiments were carried out at a static magnetic field strength of 2.35 T (100-MHz ^1H frequency) with a homemade spectrometer and probe system. Temperature control was accomplished by thermostating the spinner drive air and measuring the resulting temperature (± 1 $^{\circ}\text{C}$) close to the rotating sample via a platinum resistance sensor. A Delrin bullet-type spinner⁶ was used, with rotation speeds of about 2.4 KHz. The $\pi/2$ pulse lengths were 5–6 μs . Tropolone was obtained from Aldrich Chemical Co. and was purified by recrystallization from hexane. Exponential time constants were calculated by a least-squares program in the Nicolet NTCFT software package and are uncorrected for ^{13}C T_1 effects and ^{13}C spin diffusion contributions. ^{13}C T_1 values were measured to be quite long, ranging from more than 40 s at 28 $^{\circ}\text{C}$ to 25 s at 40 $^{\circ}\text{C}$, and were therefore neglected in the exchange calculations. Spin diffusion among ^{13}C spins has been found to be very weak in the case of rapid sample spinning.¹

Results and Discussion

The experiment used to extract exchange rates is shown schematically in Figure 4. This experiment is an example of saturation transfer or magnetization transfer, a type of experiment originally proposed by Forsen and Hoffman.⁷ In this case it is applied to the solid state and employs a special pulse sequence to prepare nonequilibrium z magnetization of the ^{13}C spins. The spectrometer transmitter frequency is adjusted to be exactly between the frequencies of C-1 and C-2 (they are the most clearly resolved resonances participating in exchange with each other). The ordinary cross-polarization sequence is carried out, but the detection that ordinarily follows this interval is replaced with a suitable evolution period, Δ_{cs} , as depicted in Figure 4. Δ_{cs} is adjusted so as to allow magnetization vectors corresponding to C-1 and C-2 to precess according to their chemical shifts in a manner that will place them along the $+x$ and $-x$ axes after this interval. In a spinning experiment, dephasing of magnetization vectors is due not only to isotropic chemical shifts but also to the time dependence of the resonance frequency resulting from the manifestation of chemical shift anisotropy (CSA) under spinning. Only at the end of each spinner period are the CSA effects refocused as rotational echoes in a MAS experiment.⁸ Hence, only for these points in time is one justified in considering only the effects of isotropic chemical shifts. Accordingly, the period Δ_{cs} was chosen to correspond to four spinner-rotation periods for the results presented in this paper. Of course, this issue is less critical for smaller magnitudes of the CSA in hertz. For experiments at low field and with resonances having small CSA in parts per million this matter can be neglected. A subsequent $(\pi/2)_y$ pulse places these components along the $+z$ and $-z$ axes. At this point the sites corresponding to C-1 and C-2 are effectively labeled with positive and negative z magnetization. The next period, Δ_m allows

(6) V. J. Bartuska and G. E. Maciel, *J. Magn. Reson.*, **42**, 312 (1981).

(7) S. Forsen and R. A. Hoffman, *J. Chem. Phys.*, **39**, 2892 (1963).

(8) M. M. Maricq and J. S. Waugh, *J. Chem. Phys.*, **70**, 3300 (1979).

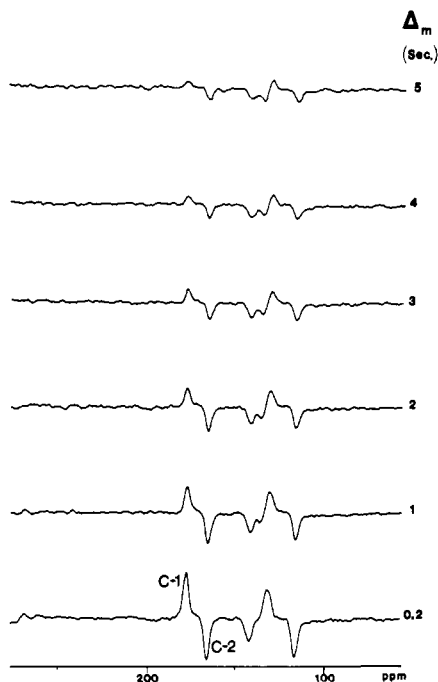


Figure 5. Plot of the ^{13}C z magnetization intensities as a function of mixing time (Δ_m) at 32 °C.

communication between these sites via chemical exchange, resulting in the net decrease of z magnetization in both sites. This decrease follows first-order kinetics and reflects the exchange rates directly. The final $\pi/2$ pulse samples this magnetization, converting it to a measurable transverse component. Phase cycling of the ^1H cross-polarization rf field, in conjunction with alternately adding and subtracting data into memory, minimizes base-line artifacts. A plot of the spectra obtained in this manner as a function of Δ_m is given in Figure 5 and can be analyzed readily to give exchange rates ($k_1 = 0.5k_{\text{NMR}}$, where k_1 is the reciprocal of the lifetime of a given carbon type and k_{NMR} is the rate for the exponential decay of magnetization in the exchange experiment). This experiment can be thought of as a particular slice in the 2-D experiment described previously, repeated for a range of mixing times, Δ_m . This exchange experiment was repeated at several temperatures to give the rate constants shown in the Arrhenius plot of Figure 6. This plot yields an activation energy of 26 ± 5 kcal/mol.

Previous studies of tropolone include several X-ray determinations of structure. The earliest was by Shimanouchi and Sasada, reporting a long C(1)–C(2) bond length of 1.452 Å but no alternation in bond length for the rest of the ring carbons.⁹ Another paper by the same authors, based on remeasured intensities, reports that there are bond-length alternations in the tropolone ring structure having the following values in angstroms: C(1)–C(2), 1.454; C(2)–C(3), 1.379; C(3)–C(4), 1.393; C(4)–C(5), 1.341; C(5)–C(6), 1.410; C(6)–C(7), 1.373; C(7)–C(1), 1.410. These values are in rough agreement with those published for 4-isopropyltropolone.¹⁰ The observation of the sharp reflections observed at 21 °C¹¹ would seem to indicate that any exchange would have to be accompanied by the subsequent relaxation of the tropolone molecule to fit back into the original lattice.

Figure 7 is a packing diagram for a tropolone molecule with its nearest neighbors as determined from the X-ray results. A proton exchange from a hydroxyl site to a carbonyl site results in a molecule that no longer has the same spacial arrangement regarding its neighbors. The only rearrangement that rectifies this situation is a rotation out of the molecular plane (out-of-plane

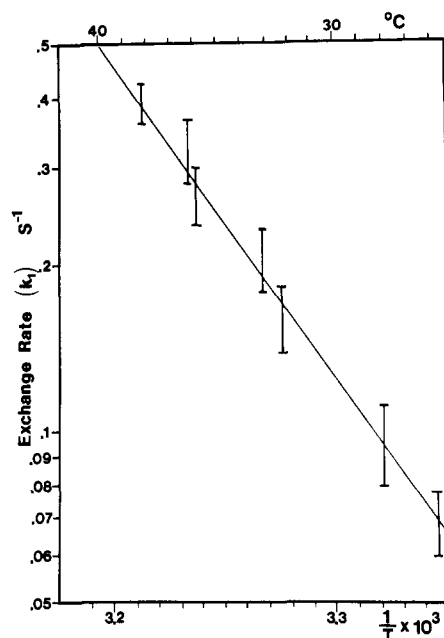


Figure 6. Arrhenius plot of exchange rate vs. $(\text{temperature})^{-1}$.

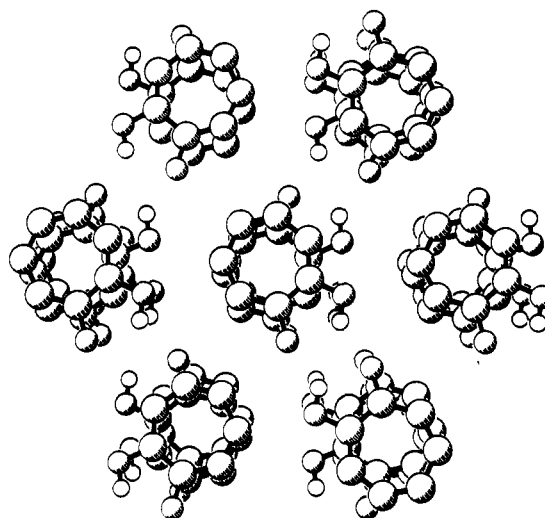


Figure 7. Packing diagram of a tropolone molecule with its nearest neighbors as determined from X-ray diffraction results.

rotation) restoring the carbonyl and hydroxyl carbons (as well as the other carbons) back to their proper lattice positions. A rotation in the plane will not accomplish this transformation. This is expected to be an energetically unfavorable process, resulting in the high activation energy of 26 kcal/mol measured in the NMR experiment.

The exchange behavior in solid tropolone has been observed before but not for the pure bulk solid and not at room temperature. Fluorescence experiments done on the tropolone monomer in a neon matrix indicate that the proton tunnels readily between the double-well minima,¹² as might be expected in the absence of any lattice perturbations. A crude estimate of less than 16 kcal for the barrier to tunnelling has been obtained from the vibrational spectrum of matrix-isolated deuterated tropolone.¹³ Solution NMR studies¹⁴ indicate that tropolone- d undergoes deuterium transfer slower than rotational motion, i.e., 10^{-10} s, but still very rapidly compared to the time scale defined by the differences in chemical shifts in the NMR experiment.

(9) H. Shimanouchi and Y. Sasada, *Tetrahedron Lett.*, 2421 (1970).

(10) T. A. Hamor and J. E. Derry, *Acta Crystallogr. Sect. B*, **B29**, 2649, (1973).

(11) H. Shimanouchi and Y. Sasada, *Acta Crystallogr. Sect. B*, **B29**, 81 (1973).

(12) R. Rossetti and L. E. Brus, *J. Chem. Phys.*, **73**, 1546 (1980).

(13) A. C. P. Alves and J. M. Hollas, *Mol. Phys.*, **23**, 927 (1972).

(14) L. M. Jackman, J. C. Trewella, and R. C. Haddon *J. Am. Chem. Soc.*, **102**, 2519 (1980).

Tropolone as a pure solid exists as dimers, as can be seen in Figure 7. The explanation given above describing the motions involved in reorienting the tropolone molecule subsequent to a proton transfer invokes the simplest possible mechanism. It cannot be determined from the present NMR data whether the proton transfer occurs intramolecularly or intermolecularly. It is possible that a concerted process involving transfer of two protons (either intra or inter) would occur for a dimer, but again both of these molecules would then have to undergo an out-of-plane rotation to pack properly in the lattice. There is no other mechanism short of translation that would restore the order necessary to produce the sharp reflections observed in the X-ray experiment. In summary, it would appear likely that proton transfer in pure solid tropolone occurs very rapidly via a tunneling mechanism as is observed in matrix-isolated molecules but requires a subsequent energetically unfavorable reorientation to pack properly into the

crystal lattice again. It is this latter process that determines if the product will survive and is responsible for the rate of exchange measured in the current ^{13}C NMR experiment. This is also consistent with the large energy of activation, 26 kcal/mol, measured in this set of experiments.

Acknowledgment. We are grateful to Prof. O. Anderson and C. Schauer for their help and use of the Nicolet R3m/E X-ray structure determination package for the graphics on which the packing plot was prepared. This system was purchased with funds provided by the National Science Foundation (Grant CHE 8103011). The liquid-state spectra were obtained at the Colorado State University Regional NMR Center, funded by the National Science Foundation (Grant CHE 78-18581). Partial support of this work was by the U.S. Geological Survey.

Registry No. Tropolone, 533-75-5.

Triple-Decker Sandwiches.¹ Syntheses, Reactivity, Electrochemistry, and X-ray Crystal and Electronic Structures of Bis(cyclopentadienylmetal)- μ -1,3-diborolenyl Complexes with 29-34 Valence Electrons

Joseph Edwin,^{2a} Manfred Bochmann,^{2a} Michael C. Böhm,^{2b} David E. Brennan,^{2d} William E. Geiger,^{*2d} Carl Krüger,^{*2c} Jürgen Pebler,^{2a} Hans Pritzkow,^{2b} Walter Siebert,^{*2b} Wolfgang Swiridoff,^{2b} Hubert Wadepohl,^{2b} Johannes Weiss,^{2b} and Ulrich Zenneck^{2b}

Contribution from the Fachbereich Chemie der Universität Marburg, D-3550 Marburg, Federal Republic of Germany, the Anorganisch-Chemisches Institut der Universität and the Organisch-Chemisches Institut der Universität Heidelberg, D-6900 Heidelberg, Federal Republic of Germany, the Max-Planck-Institut für Kohlenforschung, D-4330 Mülheim, Federal Republic of Germany, and the Department of Chemistry, University of Vermont, Burlington, Vermont 05405. Received September 3, 1982

Abstract: The methyltetraethyl and the diethyldimethyl derivatives of the Δ^4 -1,3-diborolene heterocycle $\text{C}_2\text{B}_2\text{H}_6$, **6a,b**, were used for the synthesis of the triple-decker series $(\eta^5\text{-C}_5\text{H}_5)\text{M}(\mu\text{-C}_3\text{B}_2\text{H}_5)\text{M}'(\eta^5\text{-C}_5\text{H}_5)$, with $\text{MM}' = \text{FeCo}$, CoCo , CoNi , and NiNi (30-33 valence electrons). This was achieved either by stacking the corresponding derivatives of the sandwich complexes $(\eta^5\text{-C}_5\text{H}_5)\text{Ni}(\eta^5\text{-C}_3\text{B}_2\text{H}_5)$ (**13a,b**) or $(\eta^5\text{-C}_5\text{H}_5)\text{Co}(\eta^5\text{-C}_3\text{B}_2\text{H}_5)$ (**18a,b**) with the $(\text{C}_5\text{H}_5)\text{M}$ moieties ($\text{M} = \text{Fe}$, Co , Ni) or by the reaction of the diborolenes with mono- and dinuclear metal complexes. The intensely colored compounds are chemically or electrolytically oxidized or reduced to the corresponding charged species. As predicted by theory the "FeCo", "CoCo⁺", and "NiNi⁻" species are diamagnetic and "FeCo⁺", "CoCo", "NiCo⁺", and "NiNi" are paramagnetic, each having one unpaired electron, whereas "NiCo" and "NiNi⁺" have two unpaired electrons. Reduction of NiCo (**15b**) with potassium produced the quadruple-decker complex $[(\eta^5\text{-C}_5\text{H}_5)\text{Co}(\mu\text{-C}_3\text{B}_2\text{H}_5)]_2\text{Ni}$ (**20b**) in high yield. The reaction between NiCo and $\text{Fe}_2(\text{CO})_9$ yielded several products: the carbonyl-bridged derivative $(\eta^5\text{-C}_5\text{H}_5)\text{Co}(\mu\text{-C}_3\text{B}_2\text{H}_5)\text{Ni}(\text{CO})_3\text{Fe}(\eta^5\text{-C}_5\text{H}_5)$ (**22a**) and the triple-deckers $(\eta^5\text{-C}_5\text{H}_5)\text{Fe}(\mu\text{-C}_3\text{B}_2\text{H}_5)\text{Co}(\eta^5\text{-C}_5\text{H}_5)$ and $(\eta^5\text{-C}_5\text{H}_5)\text{Co}(\mu\text{-C}_3\text{B}_2\text{H}_5)\text{Fe}(\text{CO})_3$. The NiNi triple-decker **14b** and $\text{Fe}_2(\text{CO})_9$ resulted in the derivatives $(\eta^5\text{-C}_5\text{H}_5)\text{M}(\mu\text{-C}_3\text{B}_2\text{H}_5)\text{Fe}(\text{CO})_3$ ($\text{M} = \text{Fe}$, Ni), $(\text{CO})_3\text{Fe}(\mu\text{-C}_3\text{B}_2\text{H}_5)\text{Ni}(\text{CO})_3\text{Fe}(\eta^5\text{-C}_5\text{H}_5)$ (**25b**), and the quadruple-decker $[(\text{CO})_3\text{Fe}(\mu\text{-C}_3\text{B}_2\text{H}_5)]_2\text{Ni}$. The isomorphous structures of FeCo, NiCo, and NiNi (**17b**, **15b**, and **14b**) determined by single-crystal X-ray diffraction studies revealed the triple-decker sandwich arrangement, in which the $(\text{C}_5\text{H}_5)\text{M}$ and $(\text{C}_5\text{H}_5)\text{M}'$ moieties are η^5 bonded to the planar (± 0.01 Å) μ -1,3-diborolenyl ligand. The distances $\text{Fe}\cdots\text{Co}$, $\text{Ni}\cdots\text{Co}$, $\text{Ni}\cdots\text{Ni}$ increase from 3.20 to 3.33 to 3.41 Å, respectively. The FeCo, NiCo, and NiNi complexes crystallize in the space group $P2_1/c$ with $a = 8.574$ (2), 8.618 (3), 8.711 (1) Å; $b = 17.030$ (4), 17.392 (4), 17.403 (1) Å; $c = 13.408$ (3), 13.334 (4), 13.385 (1) Å; $\beta = 108.33$ (1), 108.13 (3), 108.53 (1)°; $V = 1858.9$, 1899.3, 1923.8 Å³, and $Z = 4$. The electronic structures of some of the triple-decker complexes were investigated by means of semiempirical MO calculations of the INDO type. The theoretical results are compared with some of the experimental findings. The paramagnetic complexes gave ^1H NMR spectra in the 40-150 ppm range. Mössbauer measurements on FeCo and FeCo⁺ revealed parallels to the ferrocene/ferricenium couple. Magnetic measurements were carried out on several compounds, and the temperature dependence of the effective magnetic moment of $\text{FeCo}^+\text{BF}_4^-$ was studied. The redox properties of the neutral complexes were studied by the electrochemical techniques of dc and ac polarography, cyclic voltammetry, and controlled-potential coulometry. Each of the compounds can be oxidized or reduced in more than one reversible electron-transfer process. The broadest electron-transfer series was found with the dicobalt compound, which underwent three reversible electron-transfer reactions (2+/+0/-) and one irreversible one (-/2-). Phase-selective ac polarography showed that the charge-transfer reactions were very rapid, suggesting no major structural reorganizations as a function of changing the overall oxidation state of the complexes.

In 1964 the existence of the triple-decker sandwich cations $(\text{C}_5\text{H}_5)_3\text{Fe}_2^+$, $(\text{C}_5\text{H}_5)_3\text{FeNi}^+$, and $(\text{C}_5\text{H}_5)_3\text{Ni}_2^+$ in the mass spectra

of metallocenes was reported.³ Despite intensive research, the only example known today with a C_5H_5 ring in a bridging position